

**NASA TECHNICAL NOTE**



**NASA TN D-6554**

*c.1*

**NASA TN D-6554**

**LOAN COPY: RETURN  
AFWL (DOUL)  
KIRTLAND AFB, N. M**

6TH ETD  
0133419



**TRANSIENT-FORCED CONVECTION FILM  
BOILING ON AN ISOTHERMAL FLAT PLATE**

*by H. R. Nagendra*

*George C. Marshall Space Flight Center  
Marshall Space Flight Center, Ala. 35812*

**NATIONAL AERONAUTICS AND SPACE ADMINISTRATION • WASHINGTON, D. C. • NOVEMBER 1971**



0133419

1. REPORT NO. NASA TN D-6554		2. GOVERNMENT ACCESSION NO.		3. RECIPIENT'S CONTRACT NO.	
4. TITLE AND SUBTITLE Transient-Forced Convection Film Boiling on an Isothermal Flat Plate		5. REPORT DATE November 1971		6. PERFORMING ORGANIZATION CODE	
7. AUTHOR(S) H. R. Nagendra		8. PERFORMING ORGANIZATION REPORT #		10. WORK UNIT NO.	
9. PERFORMING ORGANIZATION NAME AND ADDRESS George C. Marshall Space Flight Center Marshall Space Flight Center, Alabama 35812		11. CONTRACT OR GRANT NO.		13. TYPE OF REPORT & PERIOD COVERED Technical Note	
12. SPONSORING AGENCY NAME AND ADDRESS National Aeronautics and Space Administration Washington, D. C. 20546		14. SPONSORING AGENCY CODE		15. SUPPLEMENTARY NOTES	
16. ABSTRACT <p>A new approach for the solution of transient-forced convection film boiling on an isothermal flat plate using the boundary layer model is developed. The similarity variables are used to convert the governing partial differential equations to ordinary ones. The results of numerical solutions of these ordinary equations indicate that the transient process can be classified as one-dimensional conduction, intermediate, and the steady state regions. The time required for the one-dimensional conduction and the time necessary to attain a steady state condition are obtained. The influence of interfacial shear is seen to be negligible while the Prandtl Number and the ratio <math>(C_p \Delta T / h_{fg} Pr)</math> have major influence.</p> <p>The use of local similarity approximations for the intermediate regime facilitates prediction of complete boundary layer growth. Using the ratio of time at any instant to the steady state time as abscissa, the curves representing the boundary layer growth can be merged into a single mean curve within 5 percent. Further, the analysis shows that the average rate of heat transfer during transient is 50 to 100 percent higher than those at steady state. The average rate of vapor convected away is 10 to 15 percent lower than at steady state while the average rate of accumulation to form the vapor layer is 1 to 14 times larger. Further, the total heat transferred during transient increases and the evaporation decreases for increasing values of <math>C_p \Delta T / h_{fg} Pr</math>.</p>					
17. KEY WORDS Transient Film Boiling Boundary Layer Heat Transfer Similarity and Local Similarity			18. DISTRIBUTION STATEMENT		
19. SECURITY CLASSIF. (of this report) Unclassified		20. SECURITY CLASSIF. (of this page) Unclassified		21. NO. OF PAGES 45	22. PRICE \$3.00



# TABLE OF CONTENTS

	Page
INTRODUCTION. . . . .	1
PHYSICAL MODEL . . . . .	2
FORMULATION OF THE PROBLEM . . . . .	2
ANALYSIS. . . . .	5
INTERFACE MATCHING CONDITIONS . . . . .	8
Steady State Heat Transfer. . . . .	9
Fluid Flow Relation . . . . .	10
Transient Parameters . . . . .	11
Total Heat Transferred During the Transient . . . . .	11
Evaporation Rate Expressions . . . . .	12
SOLUTIONS. . . . .	14
DISCUSSION OF RESULTS . . . . .	14
Initial Phases of Motion. . . . .	15
Motion Near Steady State . . . . .	15
Intermediate Regime and the Local Similarity . . . . .	17
CONCLUSIONS. . . . .	21
APPENDIX A: INTRODUCTION OF TRANSFORMATIONS . . . . .	35
REFERENCES . . . . .	36

## LIST OF ILLUSTRATIONS

Figure	Title	Page
1.	Physical model and coordinate system . . . . .	22
2.	Plot of $(C_p \Delta T / h_{fg} Pr)$ as a function of $C_1$ and $C_2$ . . . . .	22
3.	The transient parameters $C_1$ and $C_2$ for different $R_h$ . . . . .	23
4.	Classification of different regimes . . . . .	24
5.	Steady state time as a function of $R_h$ . . . . .	24
6.	Boundary layer growth . . . . .	25
7.	Effect of $R_h$ on velocity profiles . . . . .	26
8.	Effect of $R_h$ on temperature profiles . . . . .	27
9.	Effect of Prandtl Number on temperature profile . . . . .	27
10.	Effect of $R_h$ on boundary layer growth . . . . .	28
11.	Transient velocity profiles and effect of interfacial shear . . . . .	29
12.	Temperature transients and interfacial shear . . . . .	30
13.	Variation of $H'(0)$ with $C_1$ and $C_2$ . . . . .	31
14.	Variation of $f(1)$ with $C_1$ and $C_2$ . . . . .	32
15.	Variation of heat transfer parameter with time . . . . .	33
16.	Average heat transferred and evaporation during transient as functions of $R_h$ . . . . .	34

## DEFINITION OF SYMBOLS

Symbol	Definition
$a_1, a_2$	— Constants used in equation (14a)
$b_1, b_2$	— Constants used in equation (15b)
$C_1, C_2$	— Parameters defined in equation (5c)
$C_p$	— Specific heat at constant pressure for vapor
$f, F$	— Transformed stream functions defined in equations (5a) and (5b)
$h_{fg}$	— Latent heat of vaporization
$H$	— Transformed temperature variable
$K$	— Thermal conductivity of vapor
$L$	— Length of plate
$M$	— Rate of evaporation
$M_a$	— Rate of vapor accumulation
$M_c$	— Rate at which vapor is convected away by the liquid
$Pe$	— Peclet number $(U_\infty L/\alpha)$
$Pr$	— Prandtl number $(\nu/\alpha)$ for vapor
$q$	— Rate of heat transfer
$R$	— The ratio $\left[ \frac{\rho\mu}{(\rho\mu)_1} \right]^{\frac{1}{2}}$
$R_1$	— The ratio $(\nu/\nu_1)^{\frac{1}{2}}$

## DEFINITION OF SYMBOLS (Continued)

<u>Symbol</u>	<u>Definition</u>
$R_h$	— The ratio $(C_p \Delta T / h_{fg} Pr)$
$Re$	— Reynolds number $(U_\infty L / \nu)$ , $Re_x = (U_\infty X / \nu_\ell)$
$t, t_1$	— Time variable
$T$	— Temperature variable
$u, U$	— Velocity in the direction of flow
$v, V$	— Velocity perpendicular to the plate
$x, X$	— Independent variable in the direction of flow
$y, Y$	— Independent variable perpendicular to the plate
$\alpha$	— Thermal diffusivity
$\delta$	— Boundary layer thickness of vapor
$\Delta$	— Transformed boundary layer thickness, equation (5c).
$\Delta T$	— $(T_w - T_\infty)$
$\eta$	— Independent similarity variable, equation (5a)
$\mu$	— Dynamic viscosity
$\nu$	— Kinematic viscosity
$\rho$	— Density
$\tau$	— Shear stress, equation (10a)
$\psi$	— Stream function, equation (4a)

## DEFINITION OF SYMBOLS (Concluded)

### Subscripts

### Definition

$l$	— Liquid
S	— Steady state
tr	— Transient case
x	— Based on X
w	— Value at the surface of the plate
$\infty$	— Value at a distance far away from the plate
o	— Limiting value below which one-dimensional conduction predominates

### Superscripts

### Definition

'	— Differentiation with respect to $\eta$
—	— Average or nondimensional quantity



# TRANSIENT-FORCED CONVECTION FILM BOILING ON AN ISOTHERMAL FLAT PLATE

## INTRODUCTION

Under the starting conditions of the pumps to feed cryogenic fluids for combustion in the thrust chambers of space vehicles, the temperature associated with fluid passages causes excessive vapor formation caused by the large temperature differences between the cryogenic fluid and the surrounding walls. This sudden vapor formation often reflects in the blockage of flow referred to as "vapor lock." In turn, the NPSH of the pump will be drastically affected. For remedies to the problem, the following methods are considered:

1. Preconditioning the flow passages [1] before starting the pump. This method has been used in the missions undertaken so far.
2. The possibility of using a pump capable of handling two-phase fluids revealed that a suitable design [2] of the blades can handle vapor liquid mixture ratios up to 40 percent without seriously impairing the capabilities of the pump.
3. The circulation of the cryogenic fluid with increased velocity until the walls attain the desired temperature for a normal operation of pumps.

For space vehicles operating under low-gravity conditions for long durations and necessitating frequent restarts, methods (2) and (3) are being considered. It is evident that two-phase pumping cannot be used especially when the volume of vapor generated is large. Thus, forced convection is considered as a promising remedy.

The high temperature difference between the wall passages and the cryogenic fluids results in film boiling during the initial phase of "chill down."

The available literature on forced convection film boiling [3, 4, 5, 6] is centered around the steady state analysis while no investigation of the transient case is known to the author. However, the method of characteristics has been used to analyze the transient flow and heat transfer for forced convection in the entrance region of flat ducts [7] and for free convection on a vertical flat plate [8]. In the present work, transient-forced convection film boiling on

a flat plate is analyzed by similarity and local similarity transformation techniques. For making the problem tractable, the isothermal condition of the plate is assumed. When the external heat which soaks into the system is balanced by the heat carried away by the flowing vapor-liquid system, this assumption may be justifiable.

## PHYSICAL MODEL

Figure 1 shows the physical model and the coordinate system used in the analysis. The plate is assumed to be at a uniform temperature,  $T_w$ , above the saturation temperature of the fluid. The liquid flows over the plate with a constant velocity,  $U_\infty$ , before touching the plate and the velocity,  $U_\infty$ , far away from the plate remains unaltered throughout. The liquid in the immediate neighborhood of the heated plate vaporizes and a thin layer of vapor is formed. The formation and growth of this layer is assumed to be continuous and stable. The other assumptions include the following:

1. The liquid is at a saturation temperature far away from the plate.
2. Effects of radiation and viscous dissipation are neglected.
3. Two-dimensional laminar conditions prevail.
4. All fluid properties are invariant.
5. The order of magnitude of velocity and temperatures in the direction of flow merit consideration of boundary layer approximations.

## FORMULATION OF THE PROBLEM

Under the above set of assumptions, the equations of mass, momentum, and energy are:

1. Vapor Layer

$$\frac{\partial U}{\partial X} + \frac{\partial V}{\partial Y} = 0 \quad ,$$

$$\frac{\partial U}{\partial t_1} + U \frac{\partial U}{\partial X} + V \frac{\partial U}{\partial Y} = \nu \frac{\partial^2 U}{\partial Y^2} \quad ,$$

and

$$\frac{\partial T}{\partial t_1} + U \frac{\partial T}{\partial X} + V \frac{\partial T}{\partial Y} = \frac{1}{\alpha} \frac{\partial^2 T}{\partial Y^2} \quad .$$

2. Liquid Layer

$$\frac{\partial U_l}{\partial X} + \frac{\partial U_l}{\partial Y} = 0$$

and

$$\frac{\partial U_l}{\partial t_1} + U_l \frac{\partial U_l}{\partial X} + V_l \frac{\partial U_l}{\partial Y} = \nu_l \frac{\partial^2 U_l}{\partial Y^2} \quad .$$

Consideration of the energy equation for liquid layer is not necessary since the liquid is assumed to be at a saturation temperature. The following nondimensionalizing variables are used:

$$\left. \begin{aligned} u &= \frac{U}{U_\infty} \quad , \quad v = \frac{V}{U_\infty} \quad , \\ x &= \frac{X}{L} \quad , \quad y = \frac{Y}{L} \quad , \\ t &= t_1 \frac{U_\infty}{L} \quad , \quad Re = \frac{U_\infty L}{\nu} \quad , \\ Pr &= \frac{\nu}{\alpha} \quad , \quad Pe = Re Pr \quad , \end{aligned} \right\} \quad (1a)$$

and

$$\Delta = \frac{\delta}{L} \quad .$$

where  $\delta$  is the boundary layer thickness. Similar transformation variables for liquid layer are:

$$\begin{aligned} u_l &= \frac{U_l}{U_\infty} , \\ v_l &= \frac{V_l}{U_\infty} , \end{aligned} \tag{1b}$$

and

$$Re_l = \frac{U_\infty L}{\nu_l} .$$

The resulting equations are:

1. Vapor Layer

$$\frac{\partial u}{\partial x} + \frac{\partial v}{\partial y} = 0 , \tag{2a}$$

$$\frac{\partial u}{\partial t} + u \frac{\partial u}{\partial x} + v \frac{\partial u}{\partial y} = \frac{1}{Re} \frac{\partial^2 u}{\partial y^2} , \tag{2b}$$

and

$$\frac{\partial T}{\partial t} + u \frac{\partial T}{\partial x} + v \frac{\partial T}{\partial y} = \frac{1}{Pe} \frac{\partial^2 T}{\partial y^2} . \tag{2c}$$

## 2. Liquid Layer

$$\frac{\partial u_{\ell}}{\partial x} + \frac{\partial v_{\ell}}{\partial y} = 0 \quad (2d)$$

and

$$\frac{\partial u_{\ell}}{\partial t} + u \frac{\partial u_{\ell}}{\partial x} + v \frac{\partial u_{\ell}}{\partial y} = \frac{1}{\text{Re}_{\ell}} \frac{\partial^2 u_{\ell}}{\partial y^2} \quad (2e)$$

The boundary and initial conditions for the problem are:

$$\begin{aligned} t \leq 0 \quad u = v = 0 \quad \text{everywhere} \\ T = T_w \quad \text{at } y = 0 \\ T = T_{\infty} \quad \text{for } y > 0 \\ t > 0 \quad u = v = 0 ; T = T_w \quad \text{at } y = 0 \\ T = T_{\infty} \quad \text{at } y = \Delta \\ u_{\ell} \rightarrow 1 \quad \text{as } y \rightarrow \infty \end{aligned} \quad (3)$$

where  $\Delta$  is the vapor layer thickness.

## ANALYSIS

For impulsive start of motion on a flat plate, when there is no heat transfer the problem can be solved as an exact solution of Navier Stokes equations [9] by introducing similarity transformations. The growth of boundary layer and the flow are independent of the axial coordinate.

For forced convection film boiling under steady state conditions, similarity transformations have been found [3] in the two-phase boundary layer analysis. The solutions are independent of time and are functions of  $x$ .

In an attempt to develop the similarity transformations to describe the complete transient process the following variables are sought. The stream functions  $\Psi$  and  $\Psi_\ell$  are defined as:

1. Vapor Layer

$$u = \frac{\partial \Psi}{\partial y}$$

and

(4a)

$$v = - \frac{\partial \Psi}{\partial x} .$$

2. Liquid Layer

$$u_\ell = \frac{\partial \Psi_\ell}{\partial y}$$

and

(4b)

$$v_\ell = - \frac{\partial \Psi_\ell}{\partial x}$$

satisfy the continuity equations (2a) and (2d). The next set of variables used are

$$\eta = \frac{y}{\Delta(x, t)} ,$$

$$\Psi(x, y, t) = \Delta(x, t) f(\eta) ,$$

(5a)

and

$$\frac{T(x, y, t) - T_\infty}{(T_w - T_\infty)} = H(\eta) ,$$

and for the liquid layer,

$$\eta_{\ell} = \frac{y}{\Delta_{\ell}(x, t)}$$

and (5b)

$$\Psi_{\ell}(x, y, t) = \Delta_{\ell}(x, t) F(\eta) \quad ,$$

where<sup>1</sup>

$$\Delta(x, t) = \sqrt{2} \operatorname{Re}^{-1/2} (C_1 x + C_2 t)^{1/2} \quad (5c)$$

and

$$\Delta_{\ell}(x, t) = \sqrt{2} \operatorname{Re}_{\ell}^{-1/2} (C_1 x + C_2 t)^{1/2} \quad . \quad (5d)$$

Introducing these variables in equations (2), the following set of ordinary differential equations are obtained:

$$f''' + C_2 \eta f'' + C_1 f f'' = 0 \quad , \quad (6a)$$

$$H'' + \operatorname{Pr} (C_2 H' \eta + C_1 f H') = 0 \quad , \quad (6b)$$

and

$$F''' + C_2 \eta_{\ell} F'' + C_1 F F'' = 0 \quad . \quad (6c)$$

It should be noted that  $C_1$  and  $C_2$  are considered initially as constants with respect to the independent variables  $x$ ,  $y$ , and  $t$ . Referring to equation (5c) the variation of these parameters could be estimated. The value of zero for  $C_1$  indicates that the solutions are independent of  $x$  and represent the initial phase of the transient growth. Further, the value of  $C_2$  for  $C_1 = 0$  can be estimated a priori from the available solutions [9] as about 8.0. However, this value will be obtained from the present solutions also. For  $C_2 = 0$ , the solutions are independent of time. Hence, for steady state,  $C_2 = 0$ . Thus, the range of  $C_2$  will be from 0 to about 8.0. Similarly, the range of values of

---

1. The method of obtaining these transformations are given in Appendix A.

$C_1$  can be estimated. For a given value of  $C_p \Delta T / h_{fg} Pr$ , there is a unique value of  $C_1$  under steady state conditions. Thus, variation of  $C_1$  will be from 0 to  $b$  where  $b$  depends on the parameter  $C_p \Delta T / h_{fg} Pr$ . The boundary and initial conditions in terms of transformed variables become,

$$\eta = 0, f = f' = 0 \quad H = 1$$

$$\eta = 1, \quad H = 0$$

$$\eta_\ell \rightarrow \infty, \quad F' \rightarrow 1 \tag{7}$$

## INTERFACE MATCHING CONDITIONS

At the vapor-liquid interface, the velocity, shear stress, mass, and energy balance conditions should be satisfied. An analysis similar to steady state case [3] is carried out. The result of this interface matching under boundary layer assumptions is as follows:

1. Vapor liquid interface is represented by  $\eta = 1$  or  $\eta_\ell = R_1$ , where

$$R_1 = (\nu / \nu_\ell)^{1/2} \quad . \tag{8a}$$

2. The velocity balance yields,

$$F' (R_1) = f' (1) \quad . \tag{8b}$$

3. Shear stress matching gives

$$F'' (R_1) = R f'' (1) \quad ,$$

where

$$R = \left[ (\rho\mu) / (\rho\mu)_\ell \right]^{1/2} \quad . \tag{8c}$$



4. The continuity requirements demand,

$$F(R_1) = R_f (1) \quad . \quad (8d)$$

5. The energy balance can be written at the interface as,

$$-K \left. \frac{\partial T}{\partial Y} \right|_{Y=\delta} = \rho h_{fg} \left( U \left. \frac{\partial \delta}{\partial X} - V \right) \right|_{Y=\delta} \quad . \quad (8e)$$

The left-hand side denotes the heat transferred by conduction at the interface and the right-hand side represents the heat convected during vaporization of the liquid at the interface. The subcooling of the liquid is neglected. In terms of the transformed variables, equation (8e) becomes,

$$R_h = \frac{C_p \Delta T}{h_{fg} Pr} = \frac{C_1 f(1)}{-H'(1)} \quad . \quad (8f)$$

Thus, a unique relation exists between the constants,  $C_1$  and  $C_2$ , and the property function,  $(C_p \Delta T / h_{fg} Pr)$ . It can be noted that  $C_1$  plays the same role as  $\eta_\delta$  [3] in steady state conditions.

Since equations (6) contain  $\eta$ , the value of  $\eta_\ell$  at the interface cannot be taken as zero as in the steady state case [3]. Hence, the relation [equation (8a)] should be used. Hence, a new parameter,  $R_1$ , also appears apart from other parameters; i.e.,  $Pr$  and  $R$ .

## Steady State Heat Transfer

Under the steady state conditions, the rate of heat transfer becomes,

$$q(x) = -K \left( \frac{\partial T(X, Y)}{\partial Y} \right)_{Y=0} \quad . \quad (9a)$$

In terms of the transformed variables using  $C_2 = 0$  for steady state,

$$q(x) = \frac{-K\Delta T}{L} \text{Re}^{1/2} \frac{H_S'(0)}{\sqrt{2C_1x}} \quad . \quad (9b)$$

Defining the local heat transfer coefficient and Nusselt number as

$$h_x = \frac{q(x)}{\Delta T}$$

and

$$\text{Nu}_x = \frac{h_x X}{K} \quad , \quad (9c)$$

the expression for heat transfer relation can be:

$$\frac{\text{Nu}_x}{\text{Re}_x^{1/2}} \left( \frac{\mu}{\mu_L} \right) = \frac{-R}{\sqrt{2C_1}} H_S'(0) \quad . \quad (9d)$$

## Fluid Flow Relation

The shear stress at the plate is

$$\tau = \mu \left. \frac{\partial U}{\partial Y} \right)_{Y=0} \quad . \quad (10a)$$

In terms of the present variables under steady state, equation (10a) can be:

$$\left( \frac{\tau}{\rho U_\infty^2} \right) \text{Re}_x^{1/2} = \frac{R}{\sqrt{2C_1}} f''(0) \quad . \quad (10b)$$

## Transient Parameters

The rate of heat transfer from the plate is:

$$q(X, t_1) = -K \left. \frac{\partial T(X, Y, t_1)}{\partial Y} \right\}_{Y=0} . \quad (11a)$$

In terms of the present variables, equation (11a) becomes:

$$q(x, t) = \frac{-K\Delta T}{L} \frac{H'_{tr}(0)}{\Delta} . \quad (11b)$$

The Nusselt number in the transient region is:

$$Nu_{tr} = \frac{q(x, t)X}{\Delta T K} = -H'_{tr}(0) \frac{x}{\Delta} . \quad (11c)$$

Under the steady state conditions, the Nusselt number is given in equation (9d). The ratio of  $Nu_{tr}$  to  $Nu_S$  will be useful for comparison purposes:

$$\frac{Nu_{tr}}{Nu_S} = \frac{H'_{tr}(0)}{H'_S(0)} \left( \frac{1}{\Delta} \right) . \quad (11d)$$

A similar expression for shear stress can also be obtained.

## Total Heat Transferred During the Transient

The total heat transferred until steady state is:

$$q_{tr}(x) = \int_0^{t_S} q(x, t) dt , \quad (12a)$$

where  $t_S$  is the time necessary to reach steady state. Equation (12a), in terms of the present variables, becomes:

$$q_{tr}(x) = \frac{-K \Delta T}{L} \int_0^{t_S} \frac{H'_{tr}(0)}{\Delta} dt \quad . \quad (12b)$$

Defining an average rate of heat transfer during transient, equation (12b) becomes:

$$\bar{q}_{tr}(x) = - \frac{1}{t_S} \left( \frac{K \Delta T}{L} \right) \int_0^{t_S} \frac{H'_{tr}(0)}{\Delta} dt \quad . \quad (12c)$$

The ratio of  $\bar{q}_{tr}(x)$  to the rate of heat transfer at steady state is important in presenting the main features of transient heat transfer. The ratio, after simplification using equation (9b), becomes:

$$\frac{\bar{q}_{tr}(x)}{q(x)} = \int_0^1 \frac{H'_{tr}(0)}{\bar{\Delta} H_S'(0)} d\left(\frac{t}{t_S}\right) \quad . \quad (12d)$$

## Evaporation Rate Expressions

The rate of vapor carried away by flowing fluid is:

$$\begin{aligned} \dot{M}_c(X, t_1) &= \int_0^{\delta} \rho U dY \\ M_c(x, t) &= \rho U_{\infty} L \int_0^{\Delta} u dy \\ &= (\rho U_{\infty} L) \Delta f_{tr}(1) \quad . \end{aligned} \quad (13a)$$

The total vapor carried away during transient is:

$$M_c(x) = (\rho U_{\infty} L) \int_0^{t_S} \Delta f_{tr}(1) dt \quad .$$

Rate of evaporation at steady state is:

$$M(x) = \frac{(\rho U_{\infty} L)}{\text{Re}^{1/2}} \sqrt{2C_1 x} f_S(1) \quad . \quad (13b)$$

The average rate of vapor convected during transient is:

$$\bar{M}_c(x) = (\rho U_{\infty} L) \frac{1}{t_S} \int_0^{t_S} \Delta f_{tr}(1) dt \quad . \quad (13c)$$

The ratio of the average transient convection of vapor to the evaporation rate at steady state is:

$$\frac{\bar{M}_c(x)}{M(x)} = \int_0^1 \left[ \frac{f_{tr}(1)}{f_S(1)} \bar{\Delta} d\left(\frac{t}{t_S}\right) \right] \quad . \quad (13d)$$

Apart from the vapor convected away by the fluid, there is accumulation of vapor also which increases the boundary layer thickness. The total accumulation of vapor at any distance,  $x$ , until steady state is:

$$\begin{aligned} M_a(X) &= \rho \int_0^X dX \int_0^{\delta} dY \\ M_a(x) &= \rho L^2 \text{Re}^{-1/2} \int_0^x \sqrt{2C_1 x} dx \\ &= 0.66 \sqrt{2C_1 x} \text{Re}^{-1/2} (\rho L^2) x \quad . \end{aligned} \quad (13e)$$

The average rate of accumulation is:

$$\bar{M}_a(x) = \frac{M_a(x)}{t_{1S}} = 0.66 \sqrt{2C_1 x} \text{Re}^{-1/2} \rho U_{\infty} L \left( \frac{x}{t_S} \right) \quad . \quad (13f)$$

The ratio of average rate of accumulation during transient to the steady state evaporation rate is:

$$\frac{\overline{M}_a(x)}{M(x)} = \frac{0.66}{f_S(1) (t_S/x)} \quad (13g)$$

The evaporation of vapor will be the sum of vapor accumulated and vapor convected. The ratio of the average rate of evaporation during transient to the steady state value will be the summation,

$$\frac{\overline{M}_{tr}(x)}{M(x)} = \frac{\overline{M}_c(x)}{M(x)} + \frac{\overline{M}_a(x)}{M(x)} \quad (13h)$$

## SOLUTIONS

The set of equations (6) with boundary conditions (7) and interface matching relations (8) has been solved numerically on a digital computer for parametric values of  $C_1$  [0(0.2)1.5],  $C_2$  [0(0.5)2(1)8],  $R$ (0.1, 0.01, 0.001),  $R_1$ (10, 25, 100), and  $Pr$ (0.5, 0.65, 1.0). These ranges were selected through an a priori knowledge from steady state results [4] to yield results of practical importance. The detail of the method of numerical solution is the same as that used for steady state analysis [6].

## DISCUSSION OF RESULTS

The numerical solutions of the set of equations (6) yield different values of  $R_h$  for each set of  $C_1$  and  $C_2$ ,  $Pr$ ,  $R$ , and  $R_1$ . Representative results for  $R=0.1$ ,  $Pr=1$ , and  $R_1=25.0$  are illustrated in Figure 2 as a plot of  $R_h$  versus  $C_1$  for parametric values of  $C_2$ . It can be noted that the curve  $C_2=0$  represents the unique relation between  $R_h$  and  $C_1$  [equation (8f)] under steady state conditions. This curve is the same as the one obtained by Ito and Nishikawa [4] for boiling without subcooling. The curves for finite values of  $C_2$  indicate the transient period culminating in the starting phases of motion for  $C_1=0$ , the ordinate.

## Initial Phases of Motion

The above results are replotted in Figure 3 with  $C_1$  and  $C_2$  on the axes and  $R_h$  as the parameter. It can be observed that for small values of  $C_1$  and  $C_2$  the curves will be straight lines. Also, small values of  $C_2$  correspond to the condition near steady state while small values of  $C_1$  indicate the initial phases. By using the equation for a straight line in the initial phases as

$$C_2 = -a_1 C_1 + a_2 \quad , \quad (14a)$$

where  $a_1$  is the slope of the straight line and  $a_2$  is the intercept on the ordinate, the expression for  $\Delta$  can be put as:

$$\frac{\Delta}{\sqrt{2a_2 t}} = \left[ 1 + \frac{C_1 a_1}{a_2} \left( \frac{x}{t a_1} - 1 \right) \right]^{1/2} \quad (14b)$$

For a value of  $\frac{x}{t} = a_1$ , the boundary layer thickness becomes equal to 1 irrespective of the value of  $\frac{(C_1 a_1)}{a_2}$  and the variation of  $\Delta$  depends on only time. Thus, the value of  $a_1$  indicates when the effect of  $x$  comes into the picture. Further, for all values of  $\frac{x}{t a_1} > 1$ , the one-dimensional assumption will be made and the solution will be:

$$\Delta = \sqrt{2a_2 t} \quad . \quad (15a)$$

It should be noted that for  $x/t > a_1$ , the value of  $\Delta/\sqrt{2a_2 t}$  becomes  $> 1$ , resulting in an unrealistic situation where the boundary layer thickness becomes greater than that for  $x/t = a_1$ .

## Motion Near Steady State

A similar analysis for small values of  $C_2$  can now be made using  $C_1 = -b_1 C_2 + b_2$  as the equation for the straight line,

$$\bar{\Delta} = \frac{\Delta}{\sqrt{2b_2x}} = \left[ 1 + \left( \frac{b_1C_2}{b_2} \right) \left( \frac{t}{b_1x} - 1 \right) \right]^{1/2} . \quad (15b)$$

As before, the value of  $t/x = b_1$  indicates when the effect of  $t$  can be neglected. For values of  $(t/b_1x) > 1$ , the results give rise to steady state solutions. It can be noted, as before, that for values of  $t/x > b_1$ , the value of  $\bar{\Delta}$  becomes  $> 1$  and increases monotonically. Hence, the assumption that  $\bar{\Delta} = 1$  for all  $(t/b_1x) > 1$  will be made.

Thus, the slopes of the straight lines at the two ends of the curves in Figure 3 give the demarcating values for  $t/x$ . Figure 4 brings about these results clearly. The plot of  $t$  versus  $x$  consists of two straight lines having slopes  $1/a_1$  and  $b_1$ , respectively. For all values of  $t$  below the line  $0A$ , the solution will be given by the one-dimensional heat conduction equation. Similarly, for the region above the line  $0B$ , the steady state solutions apply. The region in between these two is called the intermediate region. Similar classification was observed in the transient analysis of free convection [8]. However, in forced convection [7], only two regimes were distinguished since fully developed velocity profiles were used in the analysis. The slopes  $a_1$  and  $b_1$  depend on the parameters  $R$ ,  $R_h$ , and  $Pr$ ; the effect of  $R_1$  being negligible. The steady state time  $(t_S)$  and the time  $(t_0)$ , below which one-dimensional conduction is predominant, depend on the parameters  $R$ ,  $R_h$ , and  $Pr$  which is shown in Figure 5. The ratio  $(t/x)$  is plotted against  $R_h$  for  $R = 0.1$  and  $0.001$  and for a  $Pr = 1.0$ . The steady state value  $(t_S/x)$  increases with increase in the value of  $R_h$  up to about 1.5 and then becomes almost horizontal. This indicates that for vapors having large heat content  $(C_p \Delta T)$  compared to the latent heat of vaporization, the steady state time becomes almost constant. However, the value of  $(t_0/x)$  increases slowly with  $R_h$ . The effect of  $R$  is shown by plotting the curves for  $R = 0.001$ . The effect is less than 1 percent for all values of  $R_h$ . Thus, the interfacial shear has negligible effect on transient film boiling in deciding the steady state time. A general observation of the figure is that the intermediate region occupies about 85 percent of the entire transient development.



Hitherto, all efforts were directed towards analyzing the problem [7, 8] for very small intervals of time and the study near the steady state. Such analyses did give the time to achieve steady state and the time indicating when the flow can be considered one dimensional. But, the method of characteristics used therein did not bring about the features of the intermediate regime.

## Intermediate Regime and the Local Similarity

It is seen already that the ratio,  $C_1/C_2$ , represents a transient parameter. To obtain the development of boundary layer thickness in the complete transient regime, Figure 6 is plotted with  $\bar{\Delta}$  as the ordinate and  $(t/x)$  as the abscissa. The construction for the boundary layer growth is illustrated for  $R_h = 1.0$ ,  $Pr = 1.0$ , and  $R = 0.1$ . Using Figure 3, the values of  $C_1$  and  $C_2$  are read off for  $R_h = 1$ . Knowing the value of  $C_1$  and  $C_2$ ,  $\Delta$  can be plotted with respect to  $(t/x)$  by the expression:

$$\bar{\Delta} = \frac{\Delta}{\sqrt{2b_2x}} = \left[ \frac{C_1}{b_2} + \left( \frac{C_2}{b_2} \frac{t}{x} \right) \right]^{1/2}, \quad (16)$$

where  $b_2$  is the steady state value of  $C_1$  ( $= 1.56$  for  $R_h = 1.0$ ). For several combinations of values of  $C_1$  and  $C_2$ , a family of curves 1.2 . . . 7 are plotted. It is obvious that none of the single curves satisfy the boundary conditions. This means that there is no similarity transformation applicable to the intermediate region. Figures 7, 8, and 9 indicate that the envelope of these curves satisfies the boundary conditions. This means that for each  $(t/x)$ , the values of  $C_1$  and  $C_2$  have to be changed to yield the necessary solution. Thus, by constructing similarity transformations that are locally valid, the solutions can be sought.

It was observed during the process of obtaining  $\bar{\Delta}$  that at a fixed value of  $(t/x)$ , a minimum of  $\bar{\Delta}$  exists and this value  $\bar{\Delta}_{\min}$  is in fact the enveloping curve obtained in Figures 7, 8, and 9. For obtaining this minimum value, equation (13) is used. For  $\bar{\Delta}_{\min}$ ,

$$\frac{\partial \bar{\Delta}}{\partial C_1} = 0$$

which gives

$$(t/x) = - \frac{\partial C_1}{\partial C_2} \quad . \quad (17)$$

Thus, a relation exists between the slope of the plots in Figure 3 with  $(t/x)$ . Similar expressions giving the values of  $(t_0/x)$  and  $(t_S/x)$  were already discussed. Now, the process of obtaining the solution can be summarized as follows: At any given time (the distance and properties of the fluid) the slope  $\left(\frac{\partial C_1}{\partial C_2}\right)$  is found from equation (14). The particular combination of  $C_1$  and  $C_2$  for a given fluid can be obtained from Figure 3 and the value of  $\bar{\Delta}$  is calculated from equation (13). By repeating the process for different  $(t/x)$ , the entire boundary layer growth can be obtained. Thus, the principle of the local similarity is used to throw more light on the aspects of intermediate regime.

The concept of local similarity is used extensively in the boundary layer theory [10]. A recent discussion of this aspect can be found in Reference 11. The essential features of this concept are that:

1. The changes on the time scale are sufficiently small so that the time derivatives in the transformed governing equations can be neglected.
2. The time variable,  $t$ , can be treated as a parameter wherever it occurs explicitly.

In the present case, for the intermediate regime,  $C_1$  and  $C_2$  become functions of  $t$  and, hence, they can be treated as parameters in solving the governing equations.

As mentioned in Reference 11, no criteria for establishing the validity of the local similarity method appear, except that the time derivative in the transformed differential equations be small. Again, the smallness is only qualitative and no a priori decision has been formulated. Thus, under the assumptions of local similarity, the entire boundary layer growth has been obtained (Fig. 6) for a representative value of  $R$ ,  $R_h$ , and  $Pr$ . The "patching together" of local solutions [10], a characteristic feature of local similarity is clearly demonstrated while constructing the curves representing the boundary layer growth in Figure 6. Similar curves for different values of

$R_h$  and  $Pr$  can be obtained. The variation of  $\bar{\Delta}$  for different values of  $R_h$  is shown plotted in Figure 10 using a nondimensional ratio of times  $(t/t_S)$  as the abscissa. This mode of using the ratio of transient time to steady state time as the abscissa suggests that only slight variations (maximum of 5 percent) exists between the several curves obtained for different  $R_h$ , and a mean curve could be plotted as shown.

Figures 7, 8, 9, 11, and 12 present the transient developments of velocity and temperature profiles. In Figure 11,  $f'$  is plotted against the independent variable,  $\eta$ , for the vapor region and  $(\eta_l - R_1)$  for the liquid region. It was seen in Figure 3 that there are several combinations of  $C_1$  and  $C_2$  which give rise to the same value of  $R_h$ . Since the value  $C_1 = 0$  represents the case of pure forced convection, the ratio  $C_1/C_2$  was chosen for presenting the results. Thus,  $C_1/C_2 = \infty$  represents the steady state solution and the positive values denote the transient conditions. Figure 11 shows one of the representative sets of velocity profiles for  $R_h = 1.0$  and  $Pr = 1.0$ . For  $C_1/C_2 = 0$ , the growth of velocity profile is the steepest and coincides with the results of Reference 9. Similarly, the steady state results,  $C_1/C_2 = \infty$ , are identical with those of References 4 and 5. The transient development of velocity profiles is clearly shown in the gradually flattening velocity profiles for  $C_1/C_2$  values = 0.015 to 0.82. The effect of interfacial shear is brought about by the plot for  $R = 0.001$ . Except very near the steady state, the effect appears negligible. The effect of  $R_1$  is less than 0.1 percent in all cases. The corresponding transient developments of temperature profiles are shown in Figure 12.

Figure 7 shows the effect of  $R_h$  on the velocity profiles near steady state and near  $(t_0/x)$  represented by values of  $C_1 = 1.0$  and 0.2. One of the interesting observations is that all the profiles asymptotically reach the forced convection profile. For small values of  $R_h$ , the velocity profile becomes almost linear in the vapor and liquid regimes. Similar features for temperature profiles are shown in Figure 8.

The effect of the Prandtl number on the temperature profiles is demonstrated in Figure 9. Only the extreme cases are illustrated for clarity. For  $C_1/C_2 = 0$  (forced convection), the effect of decreasing the Prandtl number is to decrease the boundary layer thickness. For  $C_1/C_2 = \infty$ , the

the decrease in  $Pr$  makes the profile linear. For values of  $C_1/C_2$  in between these extremes, similar observations can be made. To illustrate the results of the local heat transfer parameter and the rate of evaporation during transient, the variation of  $H'(0)$  and  $f(1)$  is studied for the parametric values of  $C_1$ ,  $C_2$ ,  $R$ , and  $Pr$ . Representative results are shown in Figures 13 and 14. The variation of  $H'(0)$  with  $C_1$  for different values of  $C_2$  is illustrated in Figure 13. The plot clearly shows a linear variation of  $H'(0)$  with  $C_1$  for each  $C_2$ . With this family of straight lines and by using Figure 3, the variation of  $H'(0)$  with  $C_1$  for various values of  $R_h$  can be obtained. Such curves for representative values of  $R_h = 0.1, 1.0, \text{ and } 2.5$  are shown which indicate a decreasing trend with respect to  $C_1$ , similar to the variation of  $C_2$  in Figure 3. A study of these curves for different values of  $R$  shows that the effect is less than 1 percent in all cases except for steady state case ( $C_2=0$ ). However, similar curves that result for various values of  $Pr$  are not shown here.

Figure 14 shows the same characteristic features as Figure 13. Further, the effect of interfacial shear on  $f(1)$  is also less than 1 percent except for  $C_2=0$ . These curves vary for different Prandtl numbers because  $R_h$  depends on  $Pr$ .

The ratio of the local heat transfer parameters at any instant of time to that at steady state [equation (11d)], as a function of  $t/t_s$ , is plotted in Figure 15 for different values of  $R_h$ . For  $t=0$ , the heat transfer coefficient goes to  $\infty$  in view of the sudden temperature increase of the plate. Through the transient process, the heat transfer coefficient remains higher than the steady state values as seen in Figure 15. For fluids of lower  $R_h$  values, the heat transfer coefficient decreases more rapidly than for the fluids with higher values of  $R_h$ .

The average rates of heat transfer and evaporation during transient as a function of  $R_h$  are shown in Figure 1b. The plots of equations (12d) and (13e) indicate that the average heat transfer rate during the transient varies from 1.5 to 2 times the steady state heat transfer rates for  $R_h$  values of 0.1 to 2.5. Thus, the heat transfer rate in transient is much higher compared to that during steady state. Further, the rate of heat transfer increases for increasing values of  $R_h$ . The plots of average rates of total evaporation, vapor convected away, and vapor accumulated presents the following:

1. The vapor convected away is 10 to 15 percent lower than that at steady state.
2. Most of the vapor formed is consumed by the developing boundary layer.
3. The average rate of vapor convected and accumulated decrease with increasing values of  $R_h$ . The rate of decrease of  $M_a/M_{st}$  is very large compared to  $M_c/M_{st}$ .
4. The average rate of evaporation during transient is 2 to 15 times that at steady state.

## CONCLUSIONS

A new approach using similarity and local similarity concepts has been adopted to obtain solutions for the boundary layer equations for transient-forced convection film boiling on an isothermal flat plate.

The entire transient regime could be classified into three regions: the one-dimensional conduction regime, intermediate region, and steady state region. Exact solutions are obtained for the initial and final phases of motion and the expressions for times demarcating these regions. Using the local similarity concept, the intermediate phase is analyzed.

The effect of interfacial shear is less than 1 percent in determining the steady state time. The parameter  $(C_p \Delta T / h_{fg} Pr)$  plays a very important role in deciding the rate of heat transfer and evaporation. Larger values of  $(C_p \Delta T / h_{fg} Pr)$  increase heat transfer and decrease evaporation.

The complete history of boundary layer growth (until steady state conditions) is obtained from the local similarity analysis. When the ratio of time at any instant to the steady state time is used, the boundary layer profiles for several values of  $R_h$  collapse to within 5 percent of a mean curve.

The average rate of heat transfer during transient is 50 to 100 percent greater than the steady state heat transfer rates while the average evaporation rate is 2 to 15 times larger. The rate of accumulation of vapor to form the boundary layer gives the major contribution to the total evaporation. It varies from 1 to 14 times the steady state value. The rate of vapor convected away is about 10 to 15 percent smaller than the steady state values.

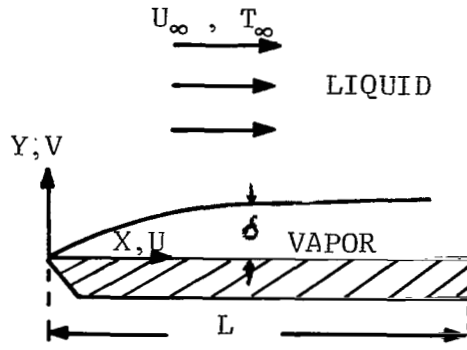


Figure 1. Physical model and coordinate system.

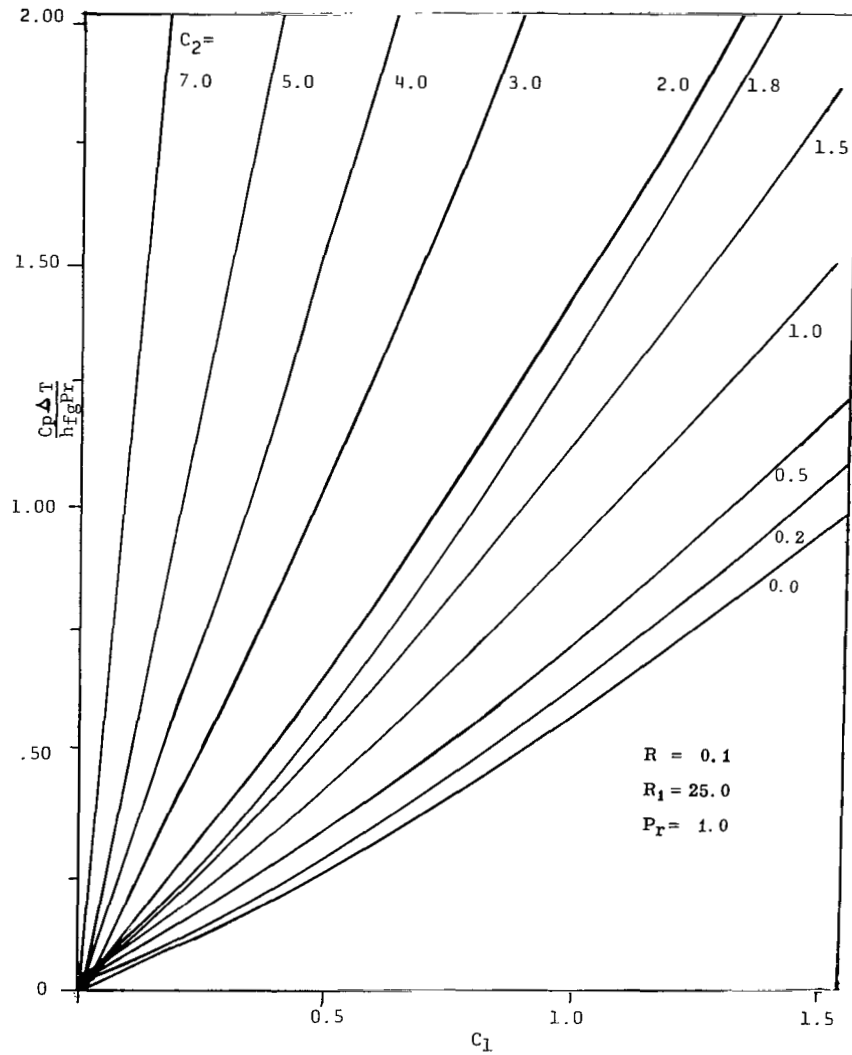


Figure 2. Plot of  $(C_p \Delta T / h_{fg} Pr)$  as a function of  $C_1$  and  $C_2$ .

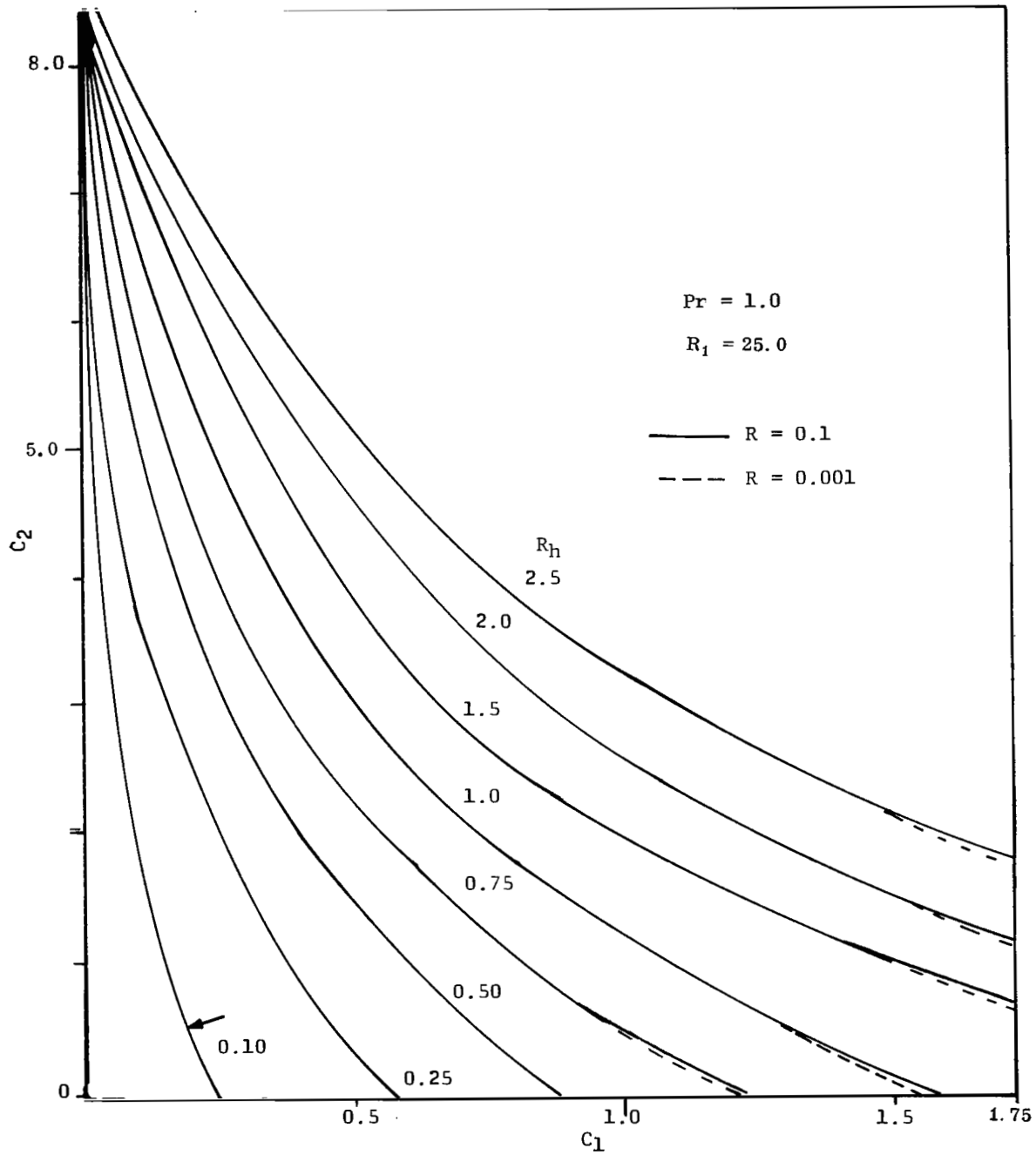


Figure 3. The transient parameters  $C_1$  and  $C_2$  for different  $R_h$ .

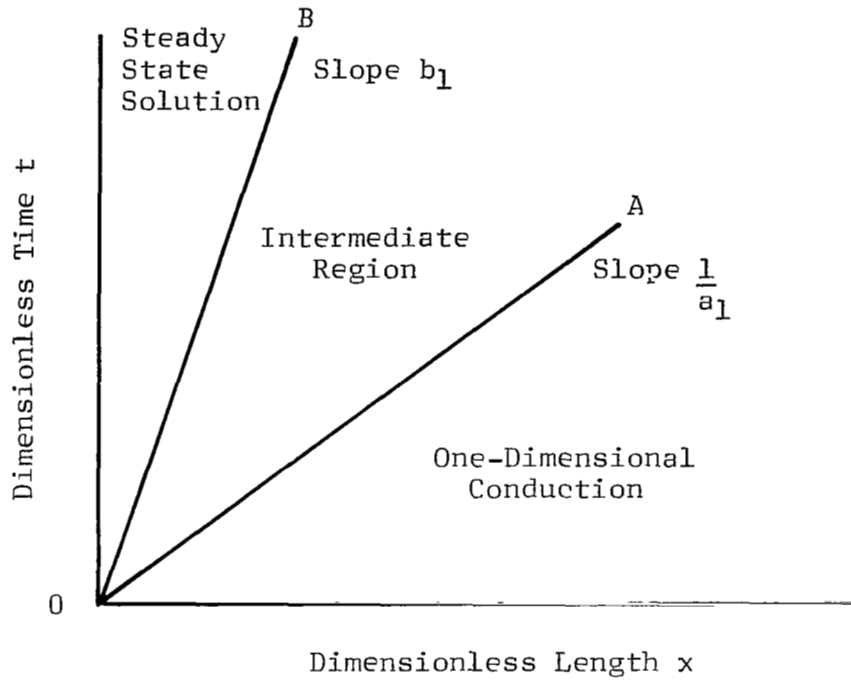


Figure 4. Classification of different regimes.

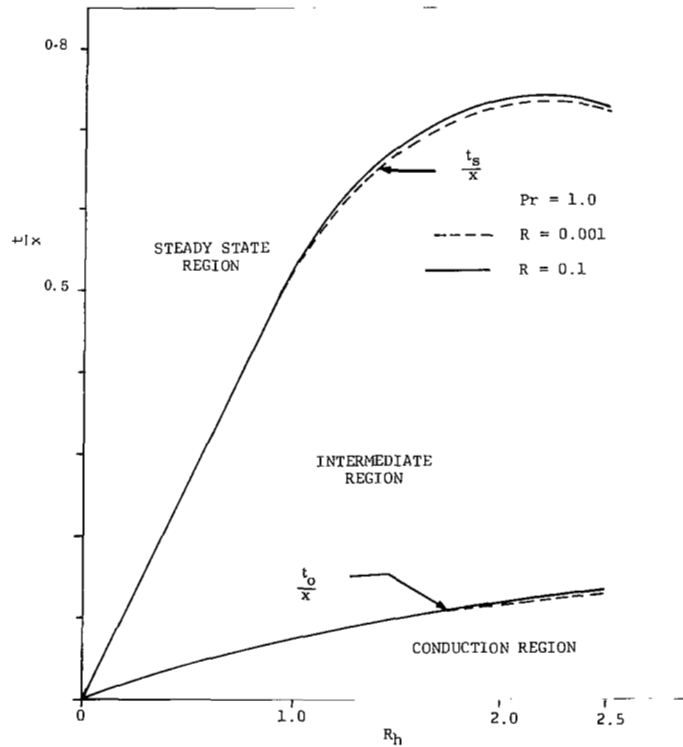


Figure 5. Steady state time as a function of  $R_h$ .



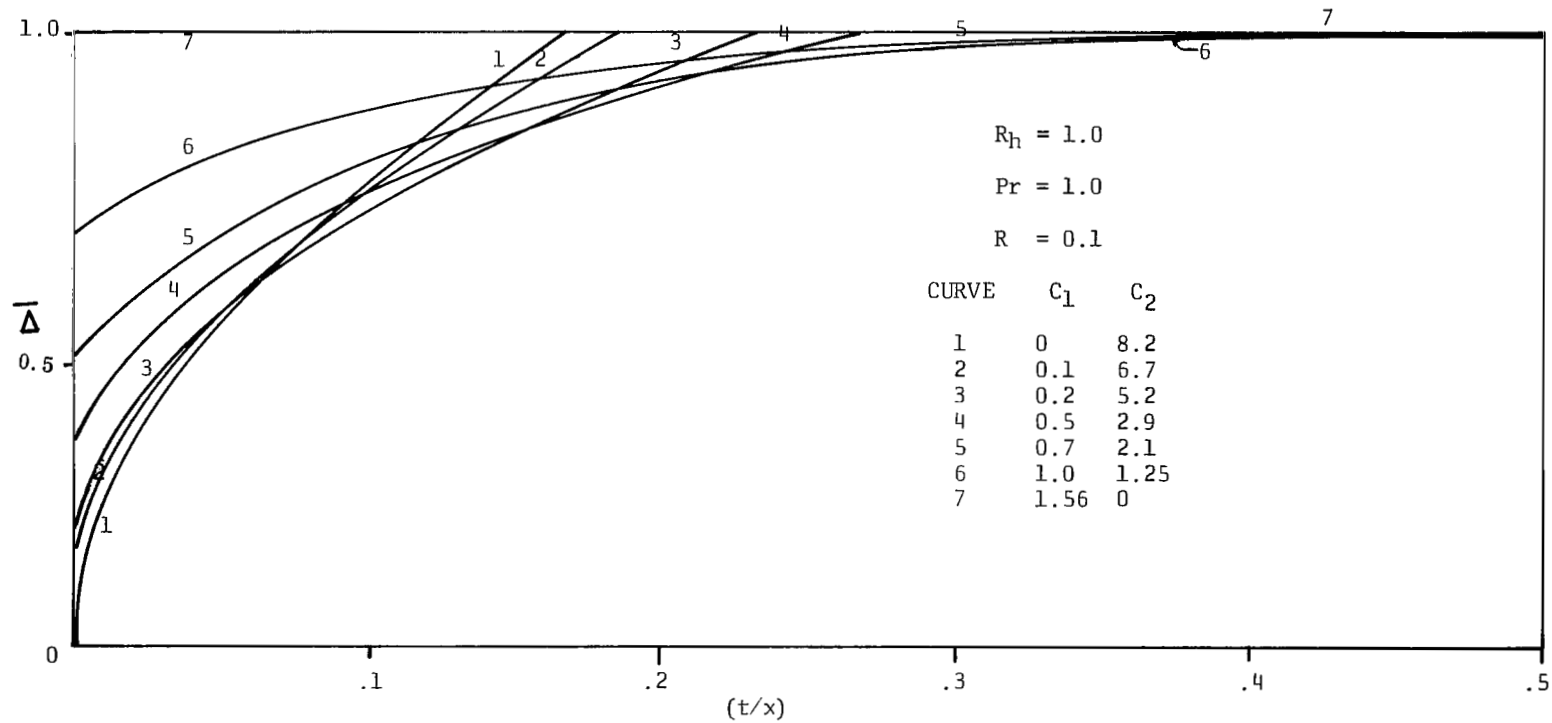


Figure 6. Boundary layer growth.

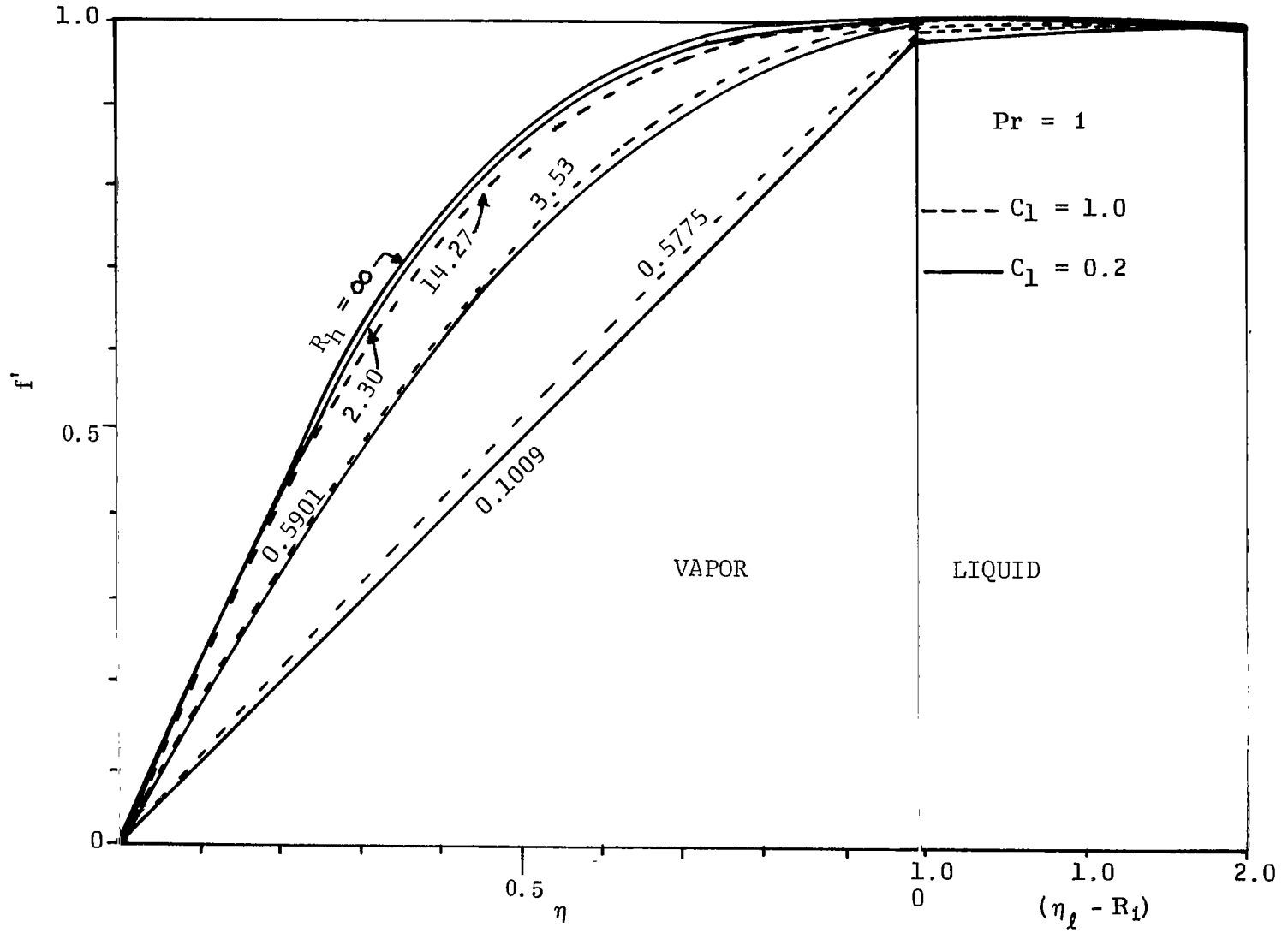


Figure 7. Effect of  $R_h$  on velocity profiles.

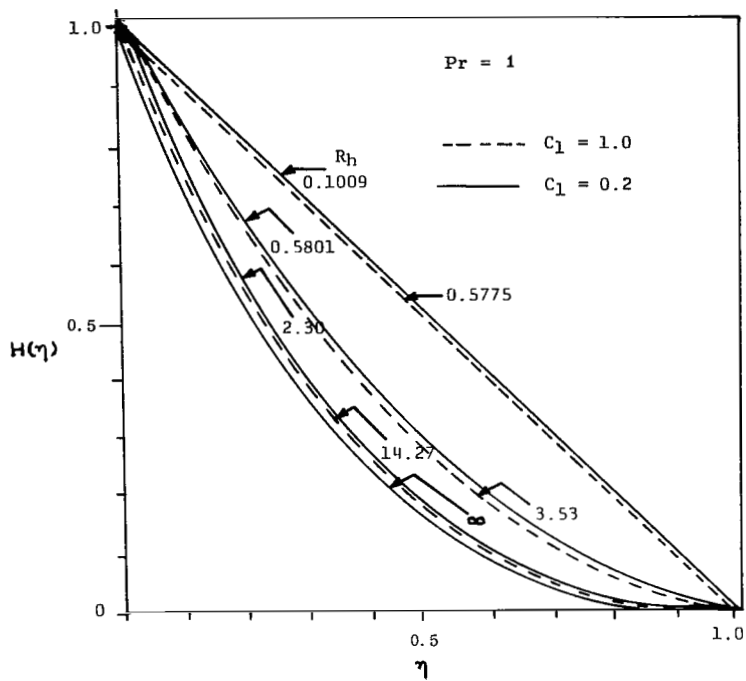


Figure 8. Effect of  $R_h$  on temperature profiles.

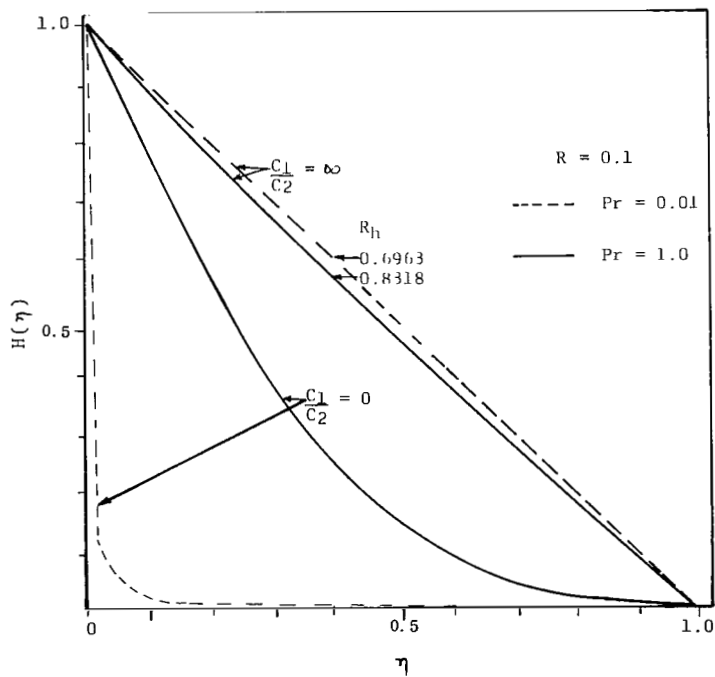


Figure 9. Effect of Prandtl Number on temperature profile.

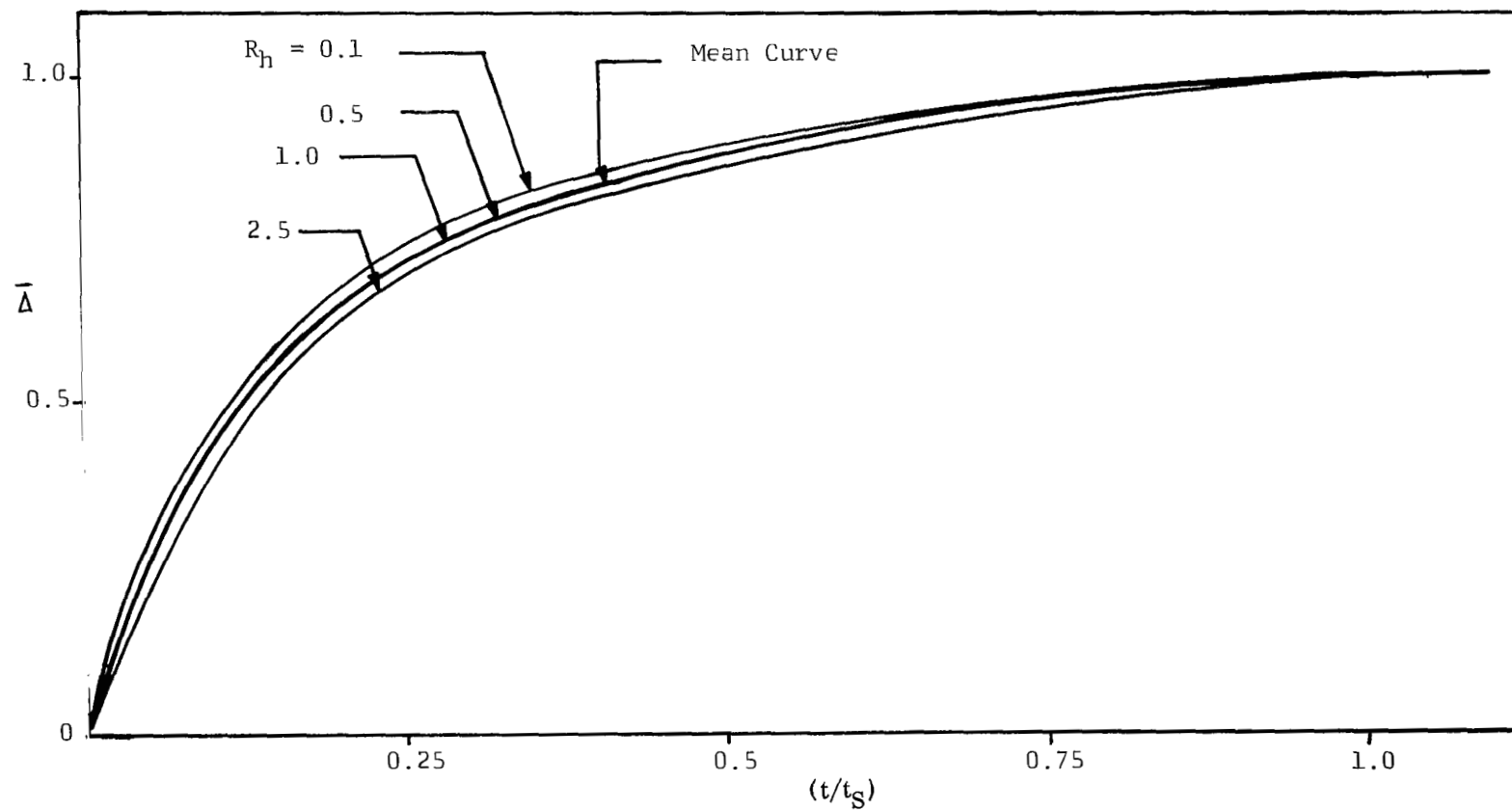


Figure 10. Effect of  $R_h$  on boundary layer growth.

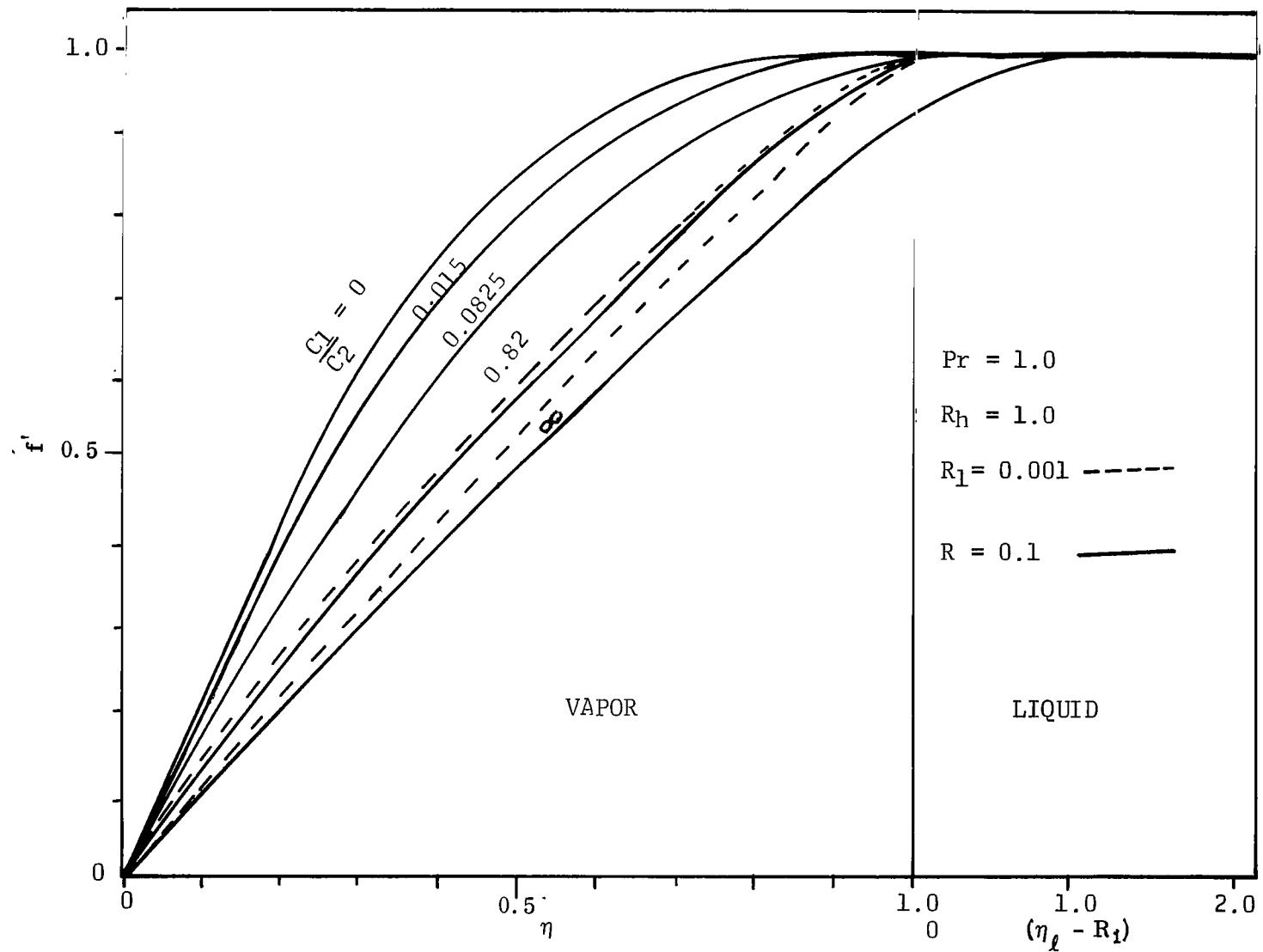


Figure 11. Transient velocity profiles and effect of interfacial shear.

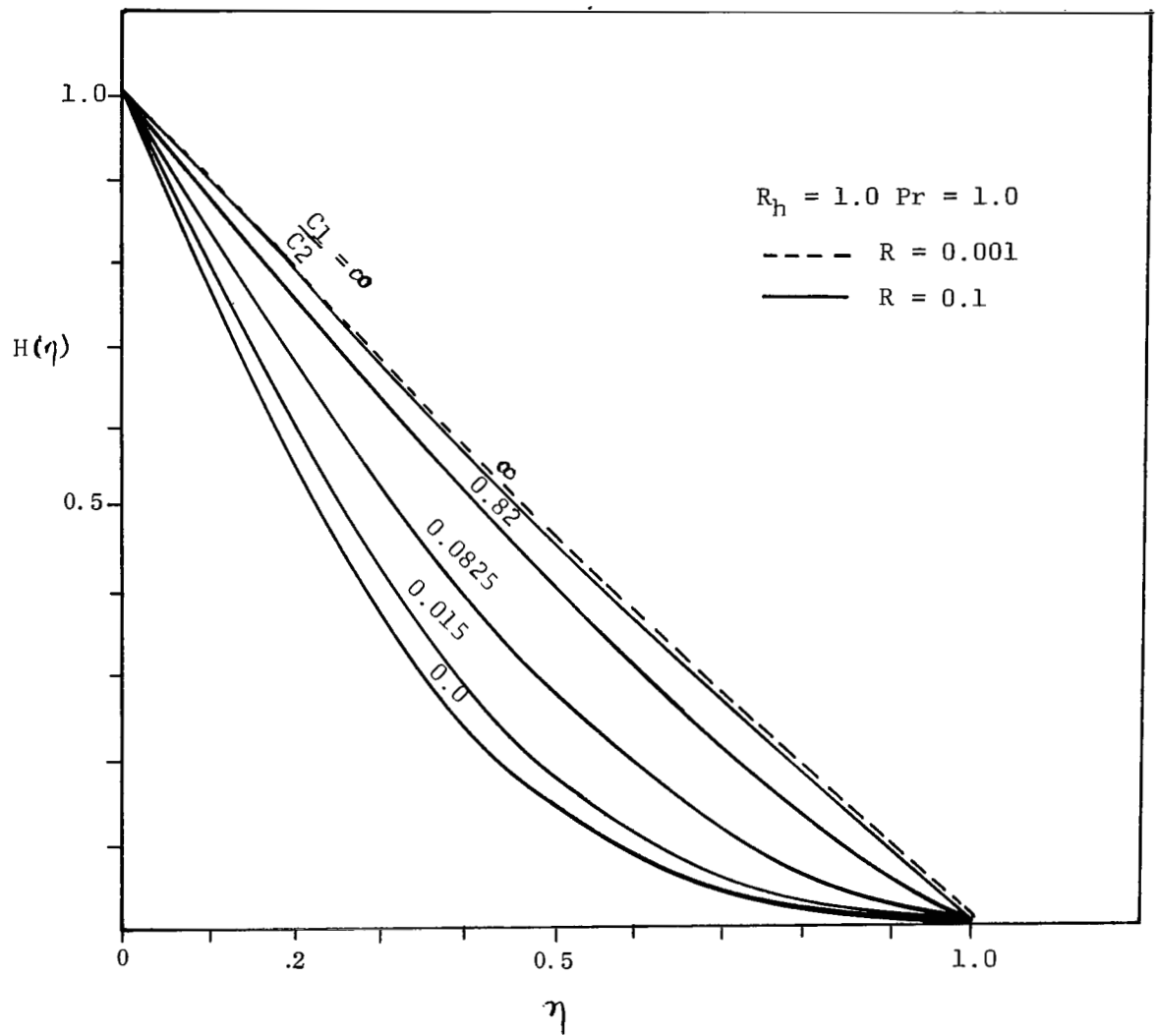


Figure 12. Temperature transients and interfacial shear.

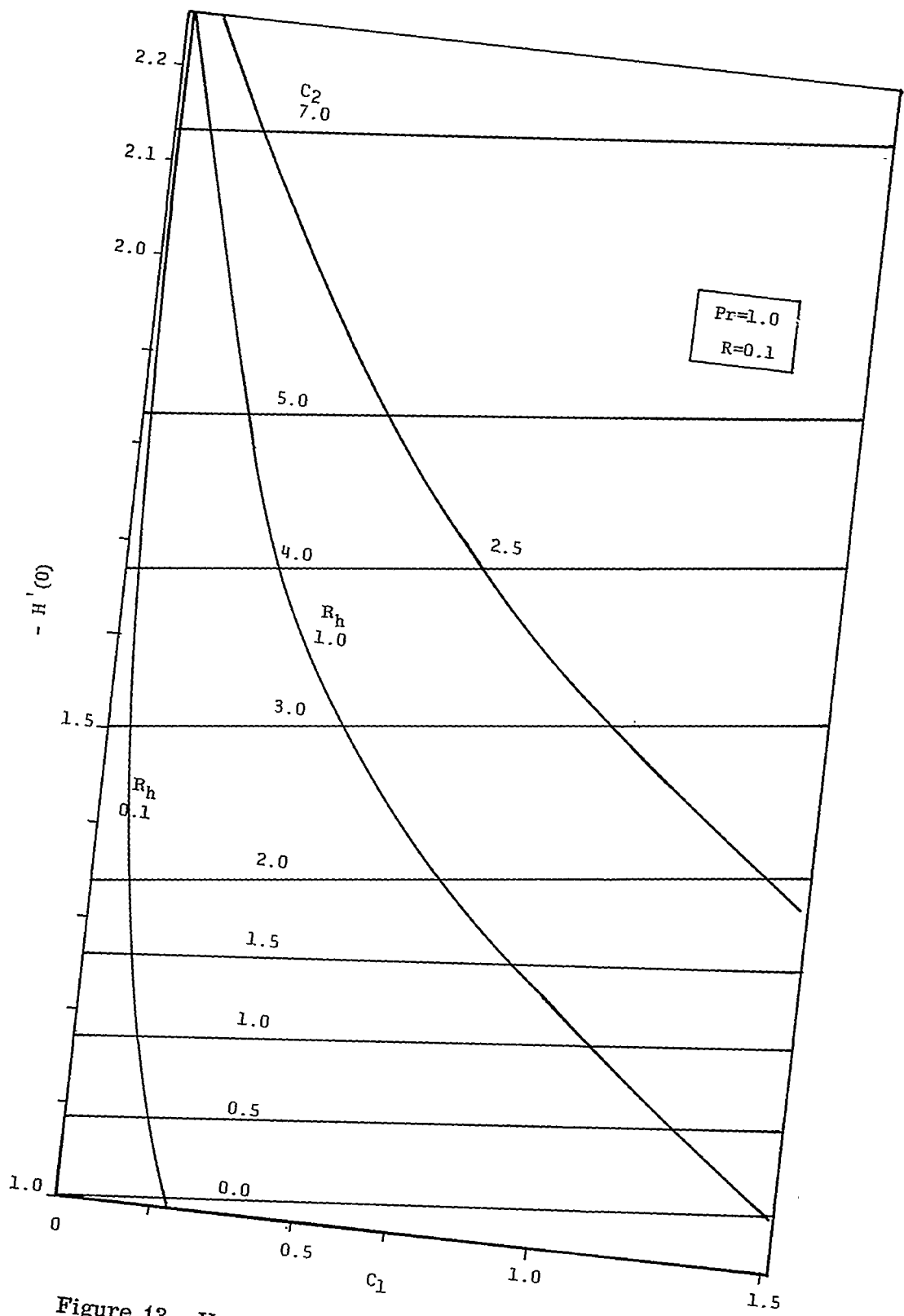


Figure 13. Variation of  $H'(0)$  with  $C_1$  and  $C_2$ .

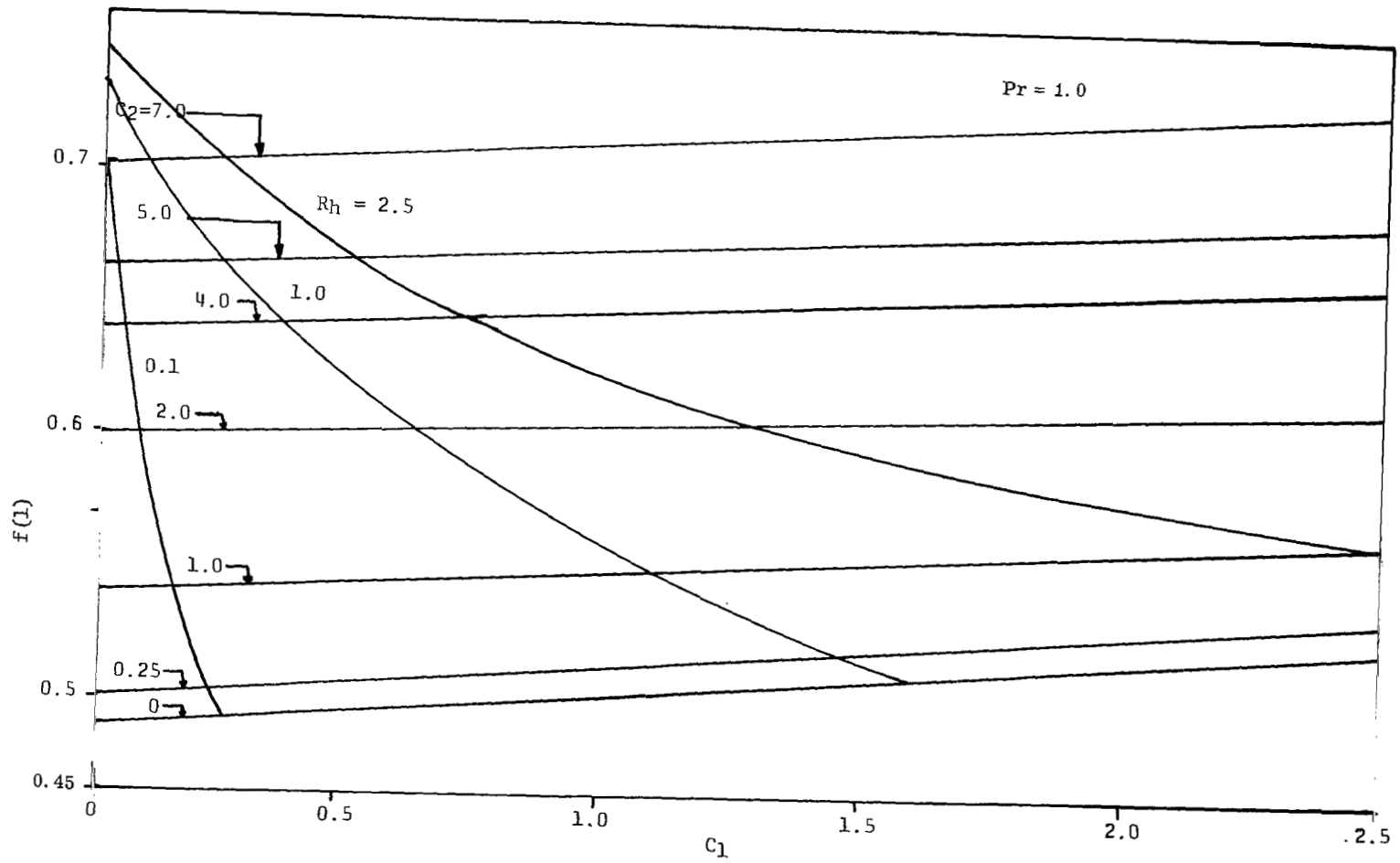


Figure 14. Variation of  $f(1)$  with  $C_1$  and  $C_2$ .



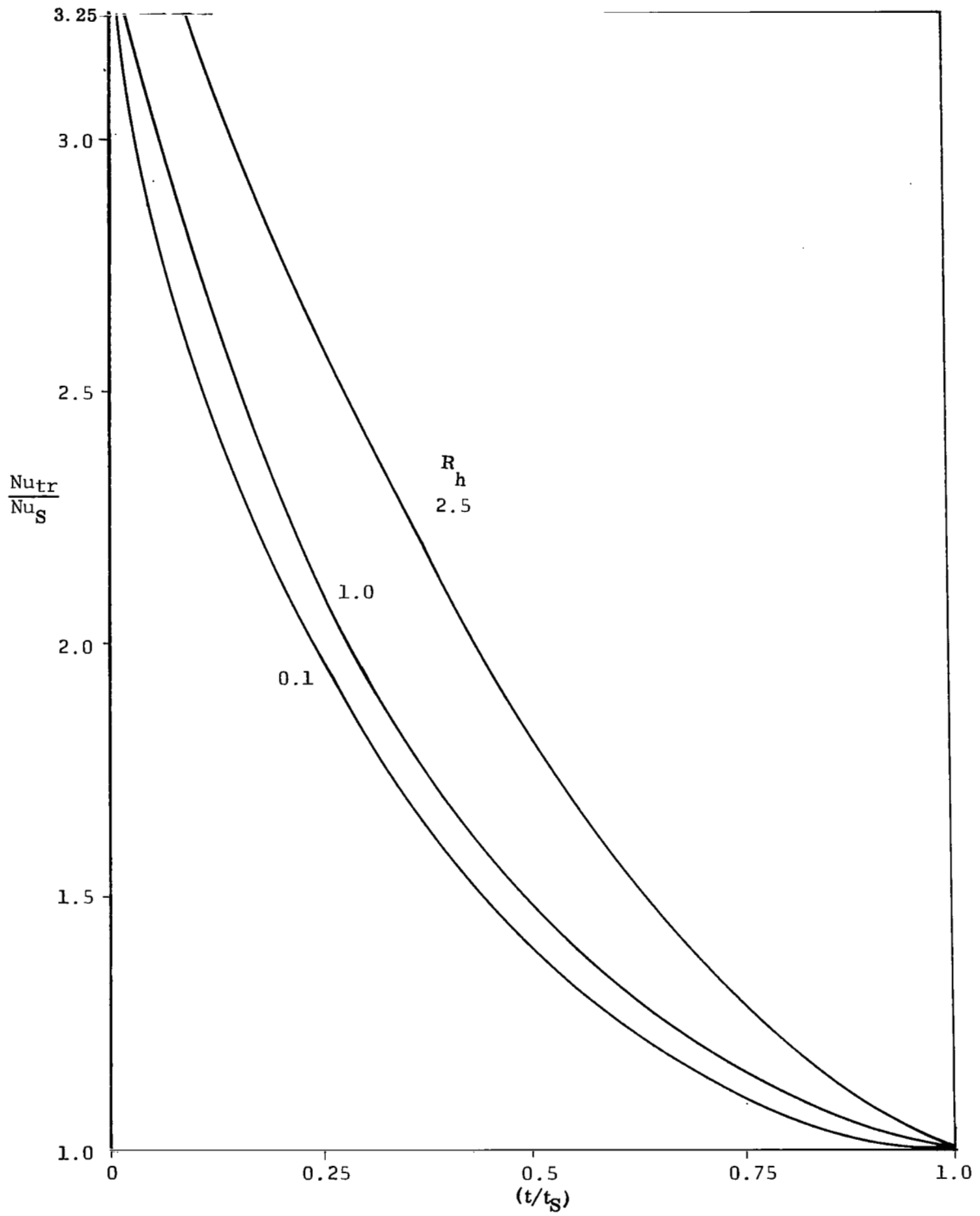


Figure 15. Variation of heat transfer parameter with time.

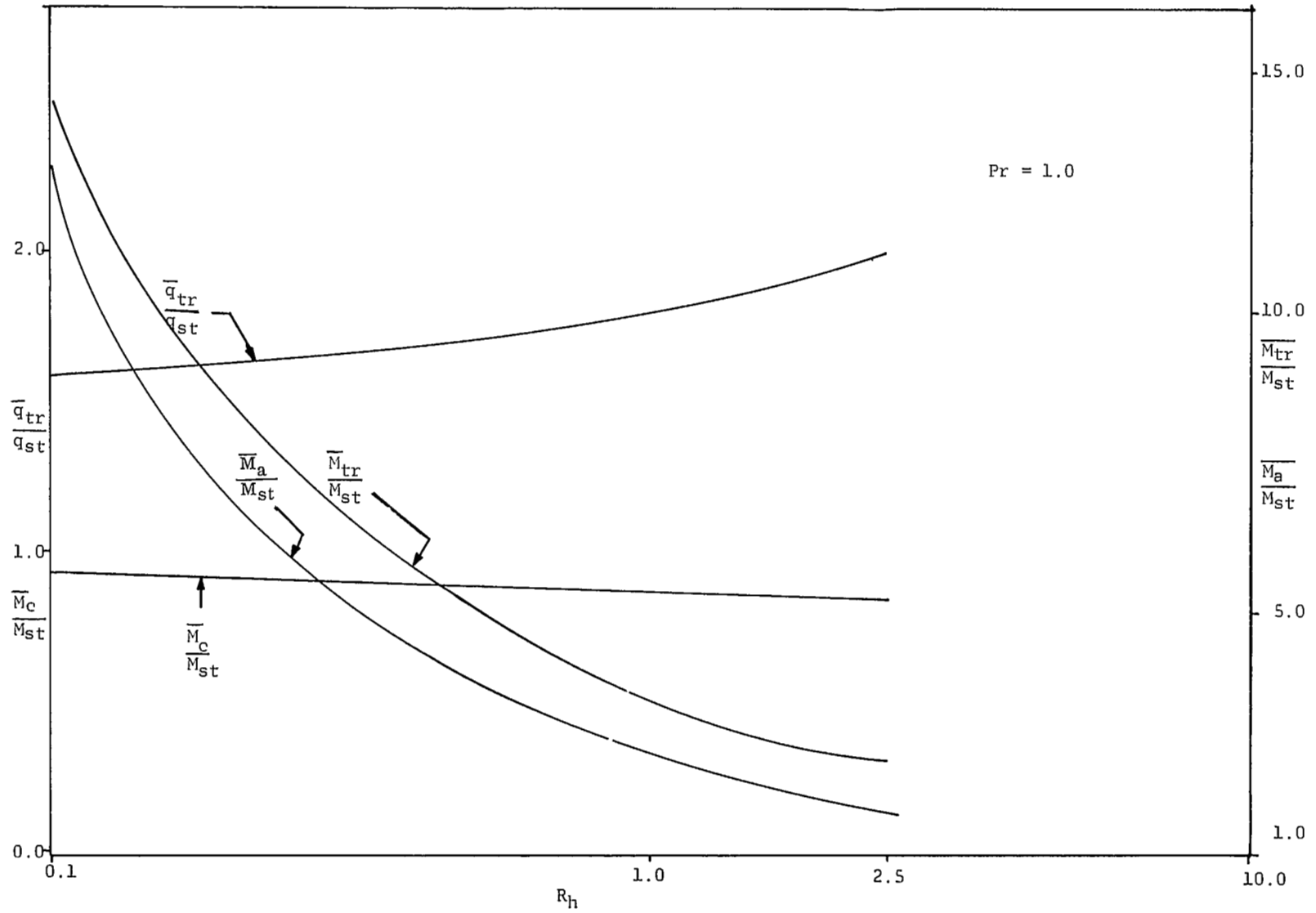


Figure 16. Average heat transferred and evaporation during transient as functions of  $R_h$ .

# APPENDIX A

## INTRODUCTION OF TRANSFORMATIONS

When the transformations in equations (5a) and (5b) are introduced into the original set of equations (2), the following partial differential equations result:<sup>1</sup>

$$f_{\eta\eta\eta} + \Delta \operatorname{Re} (\Delta_t \eta f_{\eta\eta} + \Delta_x f f_{\eta\eta}) = 0 \quad ,$$

$$H_{\eta\eta} + \Delta \operatorname{Pe} (\Delta_t \eta H_{\eta} + \Delta_x f H_{\eta}) = 0 \quad ,$$

and

$$f_{\eta\eta\eta} + \Delta_\ell \operatorname{Re}_\ell (\Delta_{t,\ell} \eta F_{\eta\eta} + \Delta_{x,\ell} F F_{\eta\eta}) = 0 \quad .$$

It can be seen that the above equations become ordinary ones if  $\Delta \Delta_t$  and  $\Delta \Delta_x$  can be made constants. These conditions resulting in two simultaneous partial differential equations can be solved to yield,

$$\Delta = (\text{constant}) (C_1 x + C_2 t)^{1/2} \quad ,$$

where again  $C_1$  and  $C_2$  are arbitrary constants. The constant outside the parenthesis is chosen as  $\sqrt{2} \operatorname{Re}^{-1/2}$  so that  $\operatorname{Re}$  does not appear explicitly in the ordinary equations. For the liquid layer,

$$\Delta_\ell = \sqrt{2} \operatorname{Re}_\ell^{-1/2} (C_1 x + C_2 t)^{1/2} \quad .$$

---

1. Subscripts  $\eta$ ,  $x$ , and  $t$  are used to denote partial differentiation with respect to those variables.

## REFERENCES

1. Booker, P. J.; Frewer, G. C.; and Pardoe, G. K. C.: Project Apollo, the Way to the Moon. American Elsevier Co. Inc., New York, 1969.
2. Bissell, W. R.; Wong, G. S.; and Winstead, T. W.: An Analysis of Two Phase Flow in LH<sub>2</sub> Pumps for O<sub>2</sub>/H<sub>2</sub> Rocket Engines. Presented at the AIAA 5th Propulsion Joint Specialists Conference, Colorado Springs, Colorado, June 9-13, 1969.
3. Cess, R. D.; and Sparrow, E. M.: Film Boiling in a Forced Convection Boundary Layer Flow. Trans. ASME, August 1961, pp. 370-376.
4. Ito, T.; and Nishikawa, K.: Two Phase Boundary Layer Treatment of Forced Convection Film Boiling. Int. J. H&M Tr., vol. 9, 1966, pp. 117-130.
5. Cess, R. D.; and Sparrow, E. M.: Subcooled Forced Convection Film Boiling on a Flat Plate. Journal Heat Tr., vol, 1961, pp. 377-379.
6. Krishnamurthy, M. V.; and Ramachandran, A.: Effect of Radiation on Film Boiling Heat Tr. Heat Tr., Soviet Research, vol. 2, 1970, pp. 1-14.
7. Siegel, R.; and Sparrow, E. M.: Transient Heat Transfer for Laminar Forced Convection in the Thermal Entrance Region of Flat Ducts. Jour. Heat Tr., 1959, pp. 29-36.
8. Siegel, R.: Transient Free Convection from Vertical Flat Plate. Tr. ASME, 1957, pp. 347-359.
9. Schlichting, H.: Boundary Layer Theory. McGraw Hill Book Co., Inc., p. 72, 1965.
10. Hayes, W. D.; and Probstein, R. F.: Hypersonic Flow Theory. First Edition, Academic Press, New York, pp. 312-316.
11. Waldman, C. E.: Theory of Heterogeneous Ignition. Comb. Science and Technology, vol. 2, 1970, pp. 81-93.



015 001 C1 U 33 711105 S00903DS  
DEPT OF THE AIR FORCE  
AF WEAPONS LAB (AFSC)  
TECH LIBRARY/WLOL/  
ATTN: E LOU BOWMAN, CHIEF  
KIRTLAND AFB NM 87117

POSTMASTER: If Undeliverable (Section 158  
Postal Manual) Do Not Return

*"The aeronautical and space activities of the United States shall be conducted so as to contribute . . . to the expansion of human knowledge of phenomena in the atmosphere and space. The Administration shall provide for the widest practicable and appropriate dissemination of information concerning its activities and the results thereof."*

— NATIONAL AERONAUTICS AND SPACE ACT OF 1958

## NASA SCIENTIFIC AND TECHNICAL PUBLICATIONS

**TECHNICAL REPORTS:** Scientific and technical information considered important, complete, and a lasting contribution to existing knowledge.

**TECHNICAL NOTES:** Information less broad in scope but nevertheless of importance as a contribution to existing knowledge.

**TECHNICAL MEMORANDUMS:** Information receiving limited distribution because of preliminary data, security classification, or other reasons.

**CONTRACTOR REPORTS:** Scientific and technical information generated under a NASA contract or grant and considered an important contribution to existing knowledge.

**TECHNICAL TRANSLATIONS:** Information published in a foreign language considered to merit NASA distribution in English.

**SPECIAL PUBLICATIONS:** Information derived from or of value to NASA activities. Publications include conference proceedings, monographs, data compilations, handbooks, sourcebooks, and special bibliographies.

**TECHNOLOGY UTILIZATION PUBLICATIONS:** Information on technology used by NASA that may be of particular interest in commercial and other non-aerospace applications. Publications include Tech Briefs, Technology Utilization Reports and Technology Surveys.

*Details on the availability of these publications may be obtained from:*

**SCIENTIFIC AND TECHNICAL INFORMATION OFFICE  
NATIONAL AERONAUTICS AND SPACE ADMINISTRATION  
Washington, D.C. 20546**